Journal of Chromatography A, 1218 (2011) 3876–3889

Contents lists available at ScienceDirect

Journal of Chromatography A

journal homepage: www.elsevier.com/locate/chroma

Optimization of startup and shutdown operation of simulated moving bed chromatographic processes

Suzhou Li[a], Yoshiaki Kawajiri[b], Jörg Raisch[a,c], Andreas Seidel-Morgenstern[a,d,*]

[a] Max-Planck-Institut für Dynamik komplexer technischer Systeme, Sandtorstraße 1, D-39106 Magdeburg, Germany
[b] School of Chemical & Biomolecular Engineering, Georgia Institute of Technology, 311 Ferst Drive, Atlanta, GA 30332, USA
[c] Fachgebiet Regelungssysteme, Technische Universität Berlin, Einsteinufer 17, D-10587 Berlin, Germany
[d] Lehrstuhl für Chemische Verfahrenstechnik, Otto-von-Guericke Universität, Universitätsplatz 2, D-39106 Magdeburg, Germany

ARTICLE INFO

Article history:
Received 7 February 2011
Received in revised form 14 April 2011
Accepted 16 April 2011
Available online 28 April 2011

Keywords:
Simulated moving bed chromatography
Startup
Shutdown
Transient operation
Dynamic optimization

ABSTRACT

This paper presents new multistage optimal startup and shutdown strategies for simulated moving bed (SMB) chromatographic processes. The proposed concept allows to adjust transient operating conditions stage-wise, and provides capability to improve transient performance and to fulfill product quality specifications simultaneously. A specially tailored decomposition algorithm is developed to ensure computational tractability of the resulting dynamic optimization problems. By examining the transient operation of a literature separation example characterized by nonlinear competitive isotherm, the feasibility of the solution approach is demonstrated, and the performance of the conventional and multistage optimal transient regimes is evaluated systematically. The quantitative results clearly show that the optimal operating policies not only allow to significantly reduce both duration of the transient phase and desorbent consumption, but also enable on-spec production even during startup and shutdown periods. With the aid of the developed transient procedures, short-term separation campaigns with small batch sizes can be performed more flexibly and efficiently by SMB chromatography.

1. Introduction

Simulated moving bed (SMB) chromatography as a continuous separation technique has been attracting increasing attention since it was developed by UOP in the early 1960s. Due to significant advantages over conventional batch chromatography, it has found many applications in the last decades in petrochemical, sugar, and fine chemical industries at various production scales. Recently, SMB has been identified as a critical tool in the pharmaceutical industry, especially for the separation of enantiomers using chiral stationary phases. For more details about SMB chromatography and its related subjects, we refer the interested reader to the comprehensive review given by Rajendran et al. [1].

The SMB system is designed as a practical realization of the true moving bed (TMB) operation. The process consists of multiple identical chromatographic columns which are connected to each other to form a closed circle. The two inlets (feed and desorbent) and two outlets (extract and raffinate) divide the unit into four distinct zones fulfilling specific roles for the separation of a binary mixture of A and B. The feed and desorbent are supplied continuously, and meanwhile the less retained component A and the more retained component B are also continuously withdrawn in the raffinate and extract streams, respectively. To mimic the countercurrent movement in TMB, the positions of the four streams are periodically shifted by one column ahead in the direction of the liquid flow after a certain switching period. Due to such a cyclic switching operation along the circularly arranged columns, SMB does not reach a steady state but rather a cyclic steady state (CSS) after startup.

Operating an SMB unit for a given separation task in general undergoes startup, normal production and shutdown periods. For convenience, we refer to the startup and shutdown also as the transient processes throughout the paper. For industrial SMB applications, typically dilute products are produced over startup and shutdown stages. These transient products do not necessarily meet purity requirements specified for the normal products and thus only CSS is used for production. On the other hand, in the academic community significant research efforts also exclusively focus on CSS. Nevertheless, improving the transient performance is always advantageous for SMBs regardless of process scale. For large-volume productions where emergency situations might occur and regular maintenance of columns is indispensable, fast startup and shutdown procedures allow to resume normal

* Corresponding author at: Lehrstuhl für Chemische Verfahrenstechnik, Otto-von-Guericke Universität, Universitätsplatz 2, D-39106 Magdeburg, Germany.
Tel.: +49 391 67 18644; fax: +49 391 67 12028.
E-mail address: anseidel@vst.uni-magdeburg.de (A. Seidel-Morgenstern).

0021-9673/$ – see front matter © 2011 Elsevier B.V. All rights reserved.
doi:10.1016/j.chroma.2011.04.051

production quickly and to reduce non-productive duration. In the case of small-scale separation campaigns, very often the same SMB unit is operated repeatedly to process small batches of well-characterized mixtures of different types. This is a rather common circumstance in pharmaceutical production. In this case, the process is subject to frequent startups and shutdowns to realize product changeover. The transient operating time can be also comparable to the production time, causing a significant portion of the feed to be consumed on the transient phases. Obviously, efficient startup and shutdown strategies are particularly helpful in such case. To the best of our knowledge, however, only very few attempts in the open literature have been made to investigate the startup and shutdown problem of conventional SMB and its derivatives. Lim and Ching [2] suggested to pre-load the columns with the feed to reduce the startup time. Xie et al. [3] further enhanced this approach by developing a detailed design procedure of pre-loading and pre-elution for their tandem SMB process for insulin purification. They also designed a shutdown procedure to recover the retained insulin. Both numerical simulations and experimental validation showed satisfactory transient performance. Bae et al. [4,5] examined effects of feed concentration and flow-rate ratio on startup and steady state behaviors of SMB. Abunasser and Wankat [6] performed both startup and shutdown analyses for their single-column chromatographic analogue to SMB, considering that the analogue would be useful in short campaigns. Rodrigues et al. [7] provided a fast model-based startup procedure for their single-column apparatus used for experimentally reproducing the periodic behavior of SMB, reducing the duration of each experimental run significantly. Nevertheless, as pointed out by the authors, the scheme was not directly applicable to a real multicolumn SMB unit since such process relies on the capability of artificially generating a prescribed inlet concentration profile. In addition, although the work by Zenoni et al. [8] was devoted to the development of an on-line system to monitor the composition of the enantiomers of a chiral SMB unit, the authors also emphasized the importance of optimizing startup and shutdown. However, none of the aforementioned contributions explicitly studied the optimal startup and shutdown operation.

Recently, we have proposed a multistage optimal startup strategy for SMB [9]. A specially tailored decomposition solution algorithm was developed to address the intractable dynamic optimization problem. In this paper, we will discuss the multistage startup concept and solution approach in more detail, and extend our previous work by explicitly considering product quality constraints into the optimal startup problem. Based on a binary separation with nonlinear Langmuir isotherm, the performance of the conventional startup and the multistage schemes with and without product quality requirements will be quantitatively compared for the first time, aiming at evaluating them in a systematic manner. Furthermore, the effect of enforcing quality constraints on the optimal operating condition and startup performance is examined. Similarly, the multistage optimal shutdown problem is also studied in this paper. The performance evaluation of various shutdown strategies is performed and their pros and cons are analyzed.

We start this paper by presenting a mathematical model used to quantify the transient behavior of SMB. In Section 3, a brief overview of design methods developed for SMB chromatography is provided, followed by an introduction of the conventional transient operation. Section 4 details the new multistage optimal startup and shutdown regimes, the problem statement and the solution approach. The systematic comparison of different transient operating policies and discussion of the results obtained is given in Section 5. We end with the concluding remarks and perspectives for future work.

2. Mathematical modeling of transient operation

In order to quantitatively characterize the transient dynamics of SMB, an accurate mathematical model capable of capturing both continuous chromatographic separation and periodical port switching is needed. Such a model can be assembled from the global node balances and the dynamic models of single chromatographic columns. By considering the mass balances around the inlet and outlet nodes, one set of node equations yields:
Desorbent node:

$$Q_{IV} + Q_D = Q_I, \quad c_{i,IV}^{out} Q_{IV} = c_{i,I}^{in} Q_I \tag{1}$$

Extract node:

$$Q_I - Q_E = Q_{II}, \quad c_{i,I}^{out} = c_{i,II}^{in} = c_i^E \tag{2}$$

Feed node:

$$Q_{II} + Q_F = Q_{III}, \quad c_{i,II}^{out} Q_{II} + c_i^F Q_F = c_{i,III}^{in} Q_{III} \tag{3}$$

Raffinate node:

$$Q_{III} - Q_R = Q_{IV}, \quad c_{i,III}^{out} = c_{i,IV}^{in} = c_i^R \tag{4}$$

where Q_j ($j = I, II, III, IV$) are the four internal flow-rates, Q_D the desorbent flow-rate, Q_E the extract flow-rate, Q_F the feed flow-rate, Q_R the raffinate flow-rate, $c_{i,j}^{in}$ and $c_{i,j}^{out}$ the liquid concentrations of component i entering and leaving zone j, c_i^E and c_i^R the liquid concentrations of component i at the extract and raffinate outlets, and c_i^F the feed concentration of component i, $i = A, B$.

To model a single column the equilibrium dispersive model [11] was used. In this model the differential mass balance of component i in each column can be written as

$$\frac{\partial c_i}{\partial t} + \frac{1-\epsilon}{\epsilon}\frac{\partial q_i}{\partial t} + v\frac{\partial c_i}{\partial z} = D_{ap,i}\frac{\partial^2 c_i}{\partial z^2}, \quad i = A,\ B \tag{5}$$

with the following initial and boundary conditions

$$c_i(t,z)|_{t=t_0} = c_{i,0} \tag{6}$$

$$D_{ap,i}\left.\frac{\partial c_i}{\partial z}\right|_{z=0} - v(c_i|_{z=0} - c_i^{in}) = 0, \; D_{ap,i}\left.\frac{\partial c_i}{\partial z}\right|_{z=L} = 0 \tag{7}$$

where c_i and q_i are the concentrations of component i in the liquid and solid phases, respectively, v the interstitial liquid velocity, t the time, z the axial coordinate along the column, ϵ the total porosity of the column, L the column length, and c_i^{in} the concentration of component i at the column inlet. The model assumes a local equilibrium between the two phases. The contributions to band broadening due to axial dispersion and mass transfer resistances are lumped into the apparent dispersion coefficients $D_{ap,i}$. For simplicity, the same coefficient was assumed in this work for both components and determined by using

$$D_{ap,i} = \frac{vL}{2N_{NTP}} \tag{8}$$

with N_{NTP} being the number of theoretical plates per column. The adsorption equilibrium of the two components was characterized by the nonlinear competitive Langmuir isotherm

$$q_i(c_A, c_B) = \frac{H_i c_i}{1 + K_A c_A + K_B c_B}, \quad i = A,\ B \tag{9}$$

with H_i being the Henry constants and K_i the thermodynamic coefficients.

For the initial conditions given in Eq. (6), some additional remarks are required. If the model equations presented above are used to describe the startup behavior, the initial time t_0 denotes the starting time of a new separation campaign. When modeling the shutdown process, it should be understood as the time instance at which the shutdown operation begins. For both kinds of problems,

t_0 is assumed to be zero for convenience. Furthermore, without loss of generality it is assumed that the process is started up with clean columns and has reached CSS before shutdown. The initial concentration value $c_{i,0}$ then can be specified conveniently. Note also that such an assumption applies to both conventional and our multistage operating strategies.

The above system of coupled partial differential equations (PDEs) was discretized in space by the orthogonal collocation on finite elements (OCFE) approach and the resulting index-1 differential algebraic equations (DAEs) were then obtained and solved by using the DASPK3.1 package [12]. Here the state variables after spatial discretization are denoted by $C(t) \in \mathbb{R}^{N_C}$, which represent the concentrations in the liquid phase at the grid nodes. N_C is the number of state variables.

3. Design methods for SMBs and conventional transient operation

3.1. Review of design methods

Development of effective and reliable design procedures for SMBs has gained considerable attention in the last decades. The most straightforward way is the trial-and-error approach, where dynamic simulations of an SMB process model are performed and operating parameters are adjusted manually after each simulation run. The procedure is repeated until the given separation specifications can be satisfied. In order to avoid this time-consuming process, some short-cut design procedures have been developed. The representatives, among them, include the standing wave approach suggested by Ma and Wang [10] and the "triangle theory" proposed by Mazzotti et al. [13]. These design methodologies provide a valuable guide for SMB practitioners and are widely used in the practical development of SMB applications. However, both procedures are based on the equivalent TMB model, and the "triangle theory" neglects the effect of axial dispersion and mass transfer resistances. To overcome these limitations, alternative model-based mathematical optimization strategies have been proposed [14–27]. They consider a detailed dynamic SMB model, involve a single or multiple objective functions, and employ efficient solution techniques well developed in the mathematical programming community. With the ability to exploit the full process potential, they have been extensively used to optimize not only the standard SMB [14,15], but also many non-standard operations, such as VariCol [16,19–21], PowerFeed [17,19,22], ModiCon [23], FF-SMB [24,25] and even the combination of different modes [18,19,26,27].

It should be noted that all the design methods reviewed above aim at determining the operating conditions fulfilling the prespecified performance criteria only at CSS, and do not take the transient performance into account. For the sake of clarity, the conditions determined are referred to as the nominal (or reference) CSS operating conditions u^*, in order to distinguish them from the transient operating conditions. Furthermore, it is assumed that u^* consists of the nominal switching period t_s^* and four dimensionless flow-rate ratios, i.e., so-called m-factors [13] defined as

$$m_j^* = \frac{Q_j^* t_s^* - \epsilon V_{Col}}{(1-\epsilon) V_{Col}}, \quad j = I, II, III, IV \tag{10}$$

with Q_j^* being the nominal CSS flow-rate in zone j, and V_{Col} the column volume. In addition, the corresponding axial concentration profile established at CSS is assumed to be unique. It exhibits a time-dependent but period-invariant behavior over each switching period. For convenience, such a steady periodic solution is denoted by $C^*(\tau) \in \mathbb{R}^{N_C}$, where $\tau \in [0, 1]$ is the dimensionless time coordinate and obtained by normalizing t with respect to t_s^*. $C^*(\tau)$ is referred to as the nominal (or reference) concentration profile. Throughout the paper, it is also assumed that u^* and $C^*(\tau)$ are known a priori.

3.2. Conventional startup operation

In the conventional operation, the SMB process is started up with clean columns and u^* is directly specified as the transient conditions, which remain constant over the entire startup stage (see Fig. 1a). One then waits until the axial concentration profile reaches its reference value. This process is schematically shown in Fig. 1c. Once at the end of some switching period, say $N_{startup}$, the corresponding axial concentration fulfills the following criterion

$$\left\| C_k|_{k=N_{startup}} - C^*|_{\tau=1} \right\|^2 \leq \epsilon_{startup} \tag{11}$$

the startup period is considered to be completed. Here $C_k \in \mathbb{R}^{N_C}$ is the axial concentration at the end of switching period k, $\epsilon_{startup}$ a pre-specified startup tolerance, and $\|\cdot\|$ the vector norm. The startup time can thus be calculated as

$$t_{startup} = N_{startup}\, t_s^* \tag{12}$$

and the total desorbent consumption follows

$$V_D^{startup} = t_{startup}\, Q_D^* \tag{13}$$

Two recovery vessels illustrated in Fig. 1c are used to contain the extract and raffinate products recovered from the outlets during the startup period, for which the purities can be defined as

$$Pu_E^{startup} = \frac{\sum_{k=1}^{N_{startup}} M_{B,k}^{startup,E}}{\sum_{k=1}^{N_{startup}} (M_{A,k}^{startup,E} + M_{B,k}^{startup,E})} \tag{14}$$

$$Pu_R^{startup} = \frac{\sum_{k=1}^{N_{startup}} M_{A,k}^{startup,R}}{\sum_{k=1}^{N_{startup}} (M_{A,k}^{startup,R} + M_{B,k}^{startup,R})} \tag{15}$$

where $M_{i,k}^{startup,E}$ and $M_{i,k}^{startup,R}$ represent the masses of component i collected over switching period k from the extract and raffinate outlets, respectively. The definition of the above parameters used to evaluate the performance of the conventional startup is also summarized in Table 1.

3.3. Conventional shutdown operation

The shutdown operation simply flushes out the holdups in the columns. Thus, it can be more aggressive than the startup operation. For example, the unit can be operated in the single-pass mode where the recycling line is cut open and the holdups are purged from the desorbent supply point to the outlet. If the products are expensive, however, recovery of the residuals becomes crucial and the process must be operated carefully. In such a case, a more "conservative" shutdown regime capable of maintaining product quality should be employed.

The simplest shutdown approach is to replace the original feed tank with a desorbent tank and all the operating conditions are kept the same as those at the CSS operation (see Fig. 1b). The column configuration at CSS is also held. The shutdown phase lasts until the components retained in the columns have eluted out from the extract and raffinate outlets, which is illustrated in Fig. 1d. In this scheme, the system actually involves two desorbent streams that purge the columns simultaneously. In this paper, we restrict ourselves to the regime and refer to it as the conventional shutdown

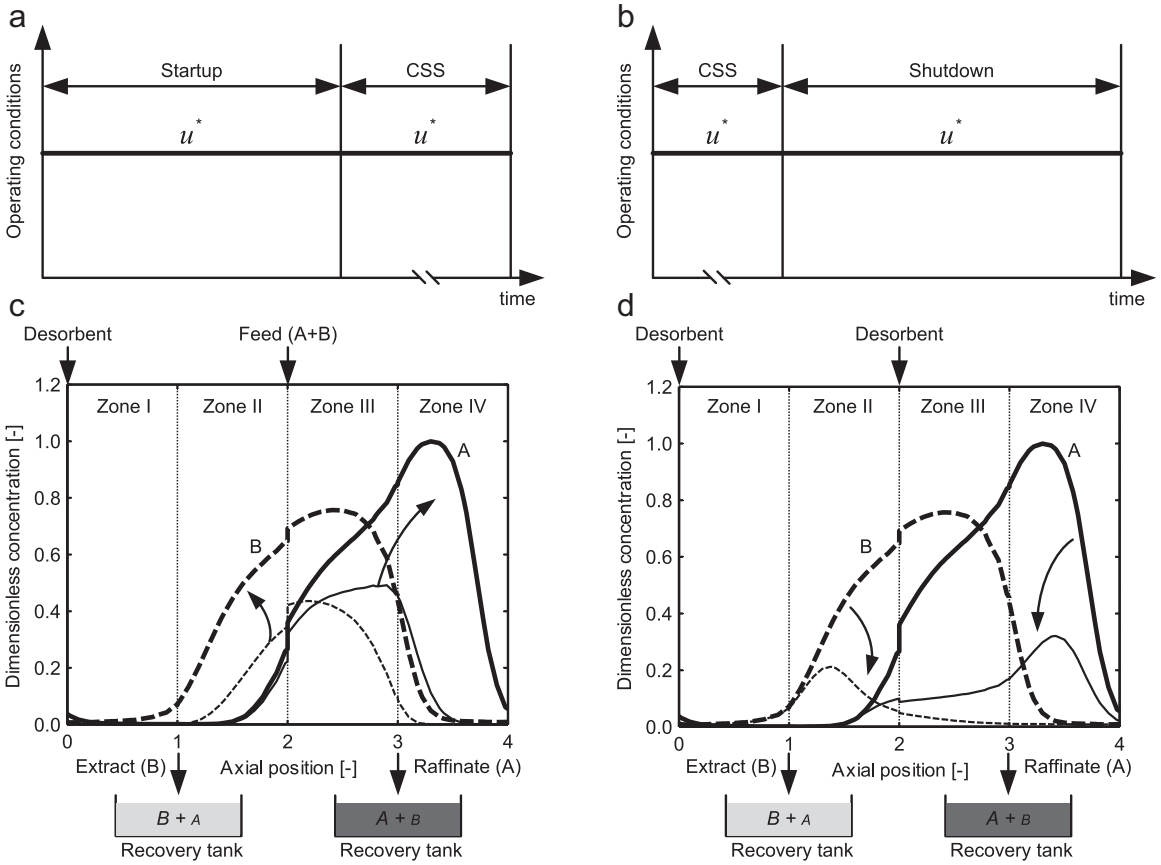

Fig. 1. Illustration of operating conditions of conventional startup (a) and shutdown (b), and development of axial concentration profiles during conventional startup (c) and shutdown (d) (taken at the end of one switching period). In (c) and (d), thin solid and dashed lines: dimensionless concentration profiles for component A and B, respectively; thick solid and dashed lines: dimensionless reference concentration profiles for component A and B, respectively. For each operating scheme, two recovery vessels are introduced to store transient products.

strategy. Similarly, two recovery tanks are also used to recover the components eluted during the shutdown stage. When the following recovery criteria for the two components are satisfied simultaneously, the shutdown process is defined to be concluded:

$$Re_i^{T,shutdown} = \frac{\sum_{k=1}^{N_{shutdown}} (M_{i,k}^{shutdown,E} + M_{i,k}^{shutdown,R})}{M_i^{Col}} \geq Re_{i,min}^{T,shutdown}, \quad i = A,\ B \tag{16}$$

where $Re_i^{T,shutdown}$ represents the total recovery of component i achieved after shutdown, $M_{i,k}^{shutdown,E}$ and $M_{i,k}^{shutdown,R}$ the masses of component i recovered over switching period k from the extract and raffinate ports, respectively, M_i^{Col} the total mass amount of component i retained in the columns before shutdown, $Re_{i,min}^{T,shutdown}$ the pre-specified minimum recovery requirement for component i, and $N_{shutdown}$ the number of switching periods required to shut down. A set of performance parameters for the conventional shutdown can be defined similarly and thus is presented in Table 1 directly. Note that in this case the total amount of desorbent consumption $V_D^{shutdown}$ should also take the amount supplied from the feed inlet into account.

The conventional strategies are often adopted in practical applications due to their simplicity of operation. However, simply using

Table 1
Definitions of performance parameters used to evaluate conventional and multistage optimal startup and shutdown strategies [a].

Parameter	Conventional operation	Multistage optimal operation
t_{mode} [h]	$N_{mode}\, t_s^*$	$\sum_{n=1}^{P} N_n^{mode}\, t_{s,n}^{mode}$
V_D^{mode} [ml]	if $mode = startup$:	
	$Q_D^*\, t_{startup}$	$\sum_{n=1}^{P} Q_{D,n}^{startup}\, N_n^{startup}\, t_{s,n}^{startup}$
	if $mode = shutdown$:	
	$(Q_D^* + Q_F^*)\, t_{shutdown}$	$\sum_{n=1}^{P} (Q_{D,n}^{shutdown} + Q_{F,n}^{shutdown})\, N_n^{shutdown}\, t_{s,n}^{shutdown}$
Product purity [%]		
Pu_E^{mode}	$\frac{\sum_{k=1}^{N_{mode}} M_{B,k}^{mode,E}}{\sum_{k=1}^{N_{mode}} (M_{A,k}^{mode,E} + M_{B,k}^{mode,E})}$	$\frac{\sum_{n=1}^{P} M_{B,n}^{mode,E}}{\sum_{n=1}^{P} (M_{A,n}^{mode,E} + M_{B,n}^{mode,E})}$
Pu_R^{mode}	$\frac{\sum_{k=1}^{N_{mode}} M_{A,k}^{mode,R}}{\sum_{k=1}^{N_{mode}} (M_{A,k}^{mode,R} + M_{B,k}^{mode,R})}$	$\frac{\sum_{n=1}^{P} M_{A,n}^{mode,R}}{\sum_{n=1}^{P} (M_{A,n}^{mode,R} + M_{B,n}^{mode,R})}$

[a] For startup operation, $mode = startup$; for shutdown operation, $mode = shutdown$.

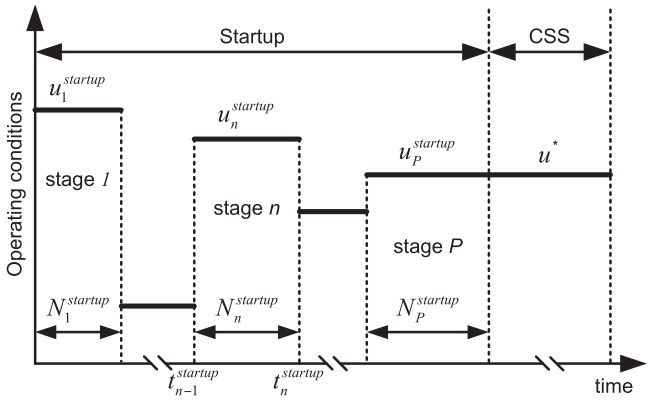

Fig. 2. Illustration of multistage startup strategy.

the CSS conditions as the transient policies typically leads to long startup and shutdown duration and a large amount of desorbent consumption. Furthermore, these approaches also suffer from another drawback that the outlet streams collected may not be necessarily guaranteed to be on-spec. In the case of off-spec production, they have to be either discarded or reprocessed. The discard scheme, although simple, causes a waste of valuable feedstock materials, which must be avoided particularly in small-scale campaigns. On the other hand, reprocessing off-spec products consumes additional production time and cost, and could be undesired for some cases. Therefore, more efficient startup and shutdown strategies which can surmount these shortcomings need to be developed.

4. Multistage optimal startup and shutdown

4.1. Multistage optimal startup strategy

The proposed multistage startup approach is schematically shown in Fig. 2. In this strategy, the startup period of interest is divided into P stages with $P \geq 1$. For the n-th stage over the time interval from $t_{n-1}^{startup}$ to $t_n^{startup}$, it is assumed that the process follows one set of time-invariant operating conditions denoted by $u_n^{startup}$, and undergoes $N_n^{startup}$ port switches ($N_n^{startup} \geq 1$), $n = 1, 2, \ldots, P$. In contrast to the conventional mode, the new startup regime allows to adjust the transient operating conditions in a stage-wise manner. Here the piece-wise constant approximation of the startup trajectory is used aiming to facilitate practical implementation, although more complex types of approximation, such as piece-wise linear or quadratic, are possible in principle. The condition $N_n^{startup} \geq 1$ guarantees the existence of stage n. Moreover, the conventional startup can be regarded as one special case of the multistage scheme, where only one stage exists with the operating conditions equal to the CSS conditions.

The primary task of a multistage optimal startup procedure is to determine $u_n^{startup}$ and $N_n^{startup}$ ($n = 1, 2, \ldots, P$) in such a way that the process can be driven from the initial conditions (i.e., clean columns) towards the reference concentration $C^*(\tau)$ in some optimum manner while respecting the constraints imposed during startup. To find the optimal startup policy, a dynamic optimization problem is required to be solved, for which the formulation and solution algorithm are detailed below.

4.1.1. Problem formulation

In stage n, the four dimensionless m-factors defined as

$$m_{j,n}^{startup} = \frac{Q_{j,n}^{startup} t_{s,n}^{startup} - \epsilon V_{Col}}{(1-\epsilon)V_{Col}}, \quad j = I, II, III, IV \tag{17}$$

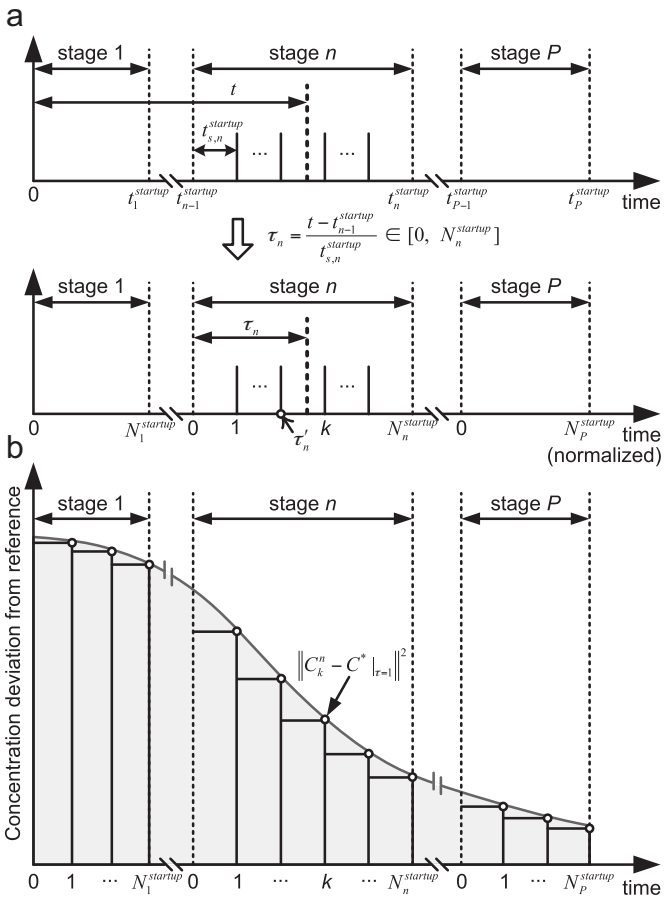

Fig. 3. (a) Transformation of time t into a local dimensionless time coordinate τ_n for stage n, and (b) development of the deviation of axial concentration from reference profile during startup and interpretation of the objective function J defined in Eq. (20) and its approximation.

and the switching period $t_{s,n}^{startup}$ are chosen as the operating conditions and thus $u_n^{startup} = \left[m_{I,\ldots,IV,n}^{startup}, t_{s,n}^{startup}\right]^T \in \mathbb{R}^5$. In Eq. (17), $Q_{j,n}^{startup}$ is the flow-rate in zone j at the n-th stage. A straightforward formulation of the objective function for a startup optimization problem is to minimize the startup time:

$$t_{startup} = \sum_{n=1}^{P} N_n^{startup} t_{s,n}^{startup} \tag{18}$$

However, selection of such objective function may lead to an ill-conditioned optimization problem. In this work, an alternative objective function was employed. For convenience of defining this objective function, a local dimensionless time coordinate τ_n is introduced for stage n:

$$\tau_n = \frac{t - t_{n-1}^{startup}}{t_{s,n}^{startup}} \in [0, N_n^{startup}] \tag{19}$$

with $t \in [t_{n-1}^{startup}, t_n^{startup}]$ and $n = 1, 2, \ldots, P$. Such a transformation is illustrated in Fig. 3a. The objective function is then defined as follows:

$$J = \sum_{n=1}^{P} t_{s,n}^{startup} \int_0^{N_n^{startup}} \left\| C^n(\tau_n) - C^*(\tau_n - \tau_n') \right\|^2 d\tau_n \tag{20}$$

where $\tau_n' = round(\tau_n)$. Here the round-to-integer function $round(\cdot)$ rounds its argument downwards to the nearest integer, and thus τ_n' represents the dimensionless starting time of a switching period

where τ_n lies (see Fig. 3a). $C^n(\tau_n) \in \mathbb{R}^{N_C}$ is the concentration state vector of stage n. In the objective function, $\left\| C^n(\tau_n) - C^*(\tau_n - \tau'_n) \right\|^2$ measures the deviation of the concentration profile from its reference value at τ_n. The development of such a deviation over the startup period is schematically illustrated in Fig. 3b by the gray line. It is easily checked that the objective function J represents the area of the shaded region in Fig. 3b. The area nicely reflects the convergence rate of the process towards the reference concentration profile. More precisely, if one set of startup conditions allows a smaller area, it implies a relatively shorter transient time and would be more preferable than others. Therefore, it is advisable to use J to characterize the startup behavior. A similar objective function was also adopted by Wozny and Li [28] for the startup optimization of distillation columns. It is worth noting that although the reference concentration profile $C^*(\tau)$ is assumed to be known, evaluating J exactly remains non-trivial since it requires the knowledge of the nominal concentration value at every $\tau \in [0, 1]$. Alternatively, the exact integration in Eq. (20) can be approximated period-wise by the rectangles depicted in Fig. 3b, yielding an approximated version $\tilde{J}$:

$$J \approx \tilde{J} = \sum_{n=1}^{P} \tilde{J}_n = \sum_{n=1}^{P} t_{s,n}^{startup} \sum_{k=1}^{N_n^{startup}} \left\| C_k^n - C^*|_{\tau=1} \right\|^2 \tag{21}$$

where $\tilde{J}_n$ denotes the approximated integral value for stage n, $C_k^n = C^n|_{\tau_n=k}$, is the value of the concentration state variables at the end of switching period k of stage n. The multistage optimal startup problem can then be formulated mathematically as follows:

$$\min_{u_n^{startup}, N_n^{startup}, n=1,\ldots,P} \tilde{J} \tag{22}$$

subject to:

$$\left\| C_{N_P^{startup}}^P - C^*|_{\tau=1} \right\|^2 \le \epsilon_{startup} \tag{23}$$

$$Pu_E^{startup} \ge Pu_{E,min}, \quad Pu_R^{startup} \ge Pu_{R,min} \tag{24}$$

$$m_{j,P}^{startup} = m_j^*, \quad t_{s,P}^{startup} = t_s^*, \qquad j = I, II, III, IV \tag{25}$$

$$Q_{I,n}^{startup} \le Q_{max}, \quad Q_{III,n}^{startup} \le Q_{max} \tag{26}$$

$$m_{I,n}^{startup} - m_{II,n}^{startup} > 0, \quad m_{I,n}^{startup} - m_{IV,n}^{startup} > 0,$$
$$m_{III,n}^{startup} - m_{II,n}^{startup} > 0, \quad m_{III,n}^{startup} - m_{IV,n}^{startup} > 0 \tag{27}$$

with $n = 1, 2, \ldots, P$. The inequality constraint in Eq. (23) requires the concentration profile at the end of stage P to approximate the reference profile within the given accuracy. The two constraints in Eq. (24) impose the purity specifications on the products recovered over startup to explicitly guarantee them to be on-spec. $Pu_{E,min}$ and $Pu_{R,min}$ are the minimum acceptable extract and raffinate purity values respectively, which are assumed to be the same as those specified for the normal products. The set of equality constraints in Eq. (25) aims to force the transient conditions at the final stage to converge to the nominal CSS conditions. The constraints in Eqs. (26) and (27) take into account the operational feasibility and restrictions that must be respected during startup. Q_{max} is the maximum allowable flow-rate in zones I and III, which is constrained typically by the capacity of the installed pumps or the pressure drop in the unit.

4.1.2. Solution strategy

Solving the problem formulated in Section 4.1.1 directly remains a significant challenge. First of all, in each stage besides the continuous operating parameters $u_n^{startup}$, an additional discrete decision variable $N_n^{startup}$ also exists because of the cyclic switching regime. This causes the original problem to be a large-scale mixed integer nonlinear programming (MINLP) problem. Furthermore, the fact that the total number of stages P is unknown a priori constitutes another serious difficulty for the direct solution approach. To deal with the numerical difficulties, a sequential decomposition algorithm has been proposed. The specially tailored solution strategy decomposes the overall problem into a sequence of stage-wise subproblems each of which can be solved relatively easier. For each sub-problem, optimizing the discrete variable $N_n^{startup}$ simultaneously may lead to further improvements in transient performance, but considerably increases the complexity of the problem. Thus, in this work, it is not treated as one degree of freedom but prespecified to reduce solution complexity, leaving the potential of optimizing also this decision variable for future work.

For stage n, the startup optimization sub-problem $Prob_n^{startup}$ is stated as below:

$$Prob_n^{startup}: \min_{u_n^{startup}} J_n^{startup} = \tilde{J}_n + \epsilon_{reg} \left\| u_n^{startup} - u^* \right\|^2 \tag{28}$$

subject to:

$$Pu_{E,n}^{startup} \ge Pu_{E,min}, \quad Pu_{R,n}^{startup} \ge Pu_{R,min} \tag{29}$$

$$Q_{I,n}^{startup} \le Q_{max}, \quad Q_{III,n}^{startup} \le Q_{max} \tag{30}$$

$$m_{I,n}^{startup} - m_{II,n}^{startup} > 0, \quad m_{I,n}^{startup} - m_{IV,n}^{startup} > 0,$$
$$m_{III,n}^{startup} - m_{II,n}^{startup} > 0, \quad m_{III,n}^{startup} - m_{IV,n}^{startup} > 0 \tag{31}$$

Note that the equality constraints in Eq. (25) cannot be considered explicitly in the above formulation. Alternatively, an additional regularizing term with the coefficient ϵ_{reg} is introduced in the objective function $J_n^{startup}$, to guide the transient conditions towards the CSS conditions as the sub-problems are solved stage by stage. This is necessary due to the non-uniqueness of the optimal solution to the above problem. As the startup proceeds, the first term $\tilde{J}_n$ becomes non-dominant and the regularizing term takes effect, leading to the convergence to u^*. Furthermore, the stage-wise purity requirements in Eq. (29) are alternatively imposed, considering that the original constraints (Eq. (24)) cannot be incorporated into this formulation directly. Here $Pu_{E,n}^{startup}$ and $Pu_{R,n}^{startup}$ represent the purities of the extract and raffinate products collected over only stage n, respectively, and are defined as

$$Pu_{E,n}^{startup} = \frac{M_{B,n}^{startup,E}}{M_{A,n}^{startup,E} + M_{B,n}^{startup,E}}, \quad Pu_{R,n}^{startup} = \frac{M_{A,n}^{startup,R}}{M_{A,n}^{startup,R} + M_{B,n}^{startup,R}} \tag{32}$$

with $M_{i,n}^{startup,E}$ and $M_{i,n}^{startup,R}$ being the masses of component i obtained over this stage from the extract and raffinate outlets, respectively. It should be pointed out that the stage-wise purity constraints provide a sufficient rather than necessary guarantee for the quality of the final products, and thus are more restrictive than the original specifications (Eq. (24)).

Once the optimal solution of the sub-problem $Prob_n^{startup}$ is found, the resulting concentration profile can be determined. Its value at the end of the stage is required to initialize that at the beginning of the next stage. The subsequent new sub-problem can then be solved once again. Such a procedure is repeated, until at the end of stage P the criterion defined in Eq. (23) is fulfilled. The decomposition algorithm described is outlined in Fig. 4. It should be stressed that the solution obtained by the algorithm is only an approximation to that of the original problem. Exploring more possibilities of refining the solution is left for our future work.

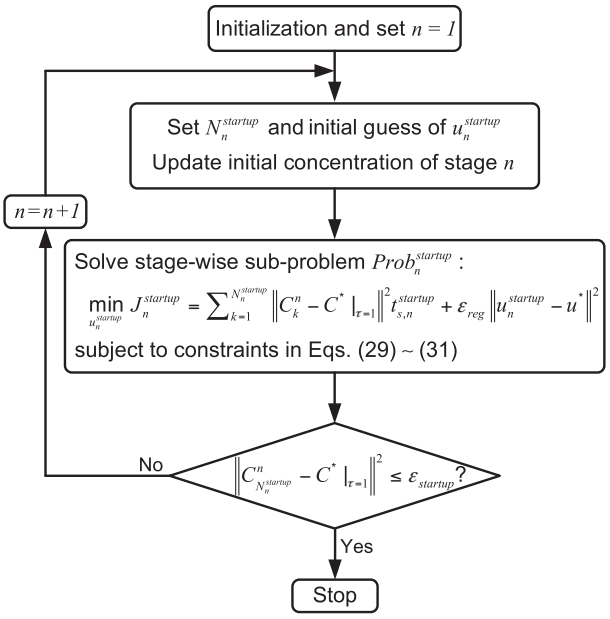

Fig. 4. Decomposition algorithm developed for solving multistage optimal startup problem.

4.2. Multistage optimal shutdown strategy

In order to overcome the limitations of the conventional shutdown operation and to enhance the shutdown performance, we have extended the multistage concept to the shutdown process, yielding a new shutdown strategy which is shown in Fig. 5. We also follow the same assumption that the SMB process has achieved a desired CSS before shutdown, as made for the conventional case. Once the shutdown begins, the original feed is replaced with a desorbent flow. Compared to the constant operating regime in the conventional mode, however, the operating conditions now are allowed to be changed stage-wise as the shutdown proceeds. It is assumed that the shutdown process lasts P stages ($P \ge 1$). For the n-stage, the transient conditions are $u_n^{shutdown}$ and $N_n^{shutdown}$ port switches are involved, $N_n^{shutdown} \ge 1$, $n = 1, 2, \ldots, P$. Finding optimal values for $u_n^{shutdown}$ and $N_n^{shutdown}$ with which the process can be shut down from the initial CSS to the final state of clean columns is the objective of a multistage optimal shutdown procedure.

The formulation of the optimal shutdown problem can be performed similar to that of the startup problem presented in Section 4.1.1 and thus is omitted here for the sake of brevity. The decomposition solution approach developed previously is also used to deal with the shutdown problem. In order to reduce the complexity of solving each sub-problem, the number of switching periods is prespecified, as treated in the startup problem. The n-th shutdown sub-problem is formulated as follows:

$$Prob_n^{shutdown}: \min_{u_n^{shutdown}} J_n^{shutdown} = \int_{t_{n-1}^{shutdown}}^{t_n^{shutdown}} \left\| C^n(t) \right\| dt \tag{33}$$

subject to:

$$Pu_{E,n}^{shutdown} \ge Pu_{E,min}, \quad Pu_{R,n}^{shutdown} \ge Pu_{R,min} \tag{34}$$

$$Q_{I,n}^{shutdown} \le Q_{max}, \quad Q_{III,n}^{shutdown} \le Q_{max} \tag{35}$$

$$m_{I,n}^{shutdown} - m_{II,n}^{shutdown} > 0, \quad m_{I,n}^{shutdown} - m_{IV,n}^{shutdown} > 0,$$
$$m_{III,n}^{shutdown} - m_{II,n}^{shutdown} > 0, \quad m_{III,n}^{shutdown} - m_{IV,n}^{shutdown} > 0 \tag{36}$$

The vector of operating conditions $u_n^{shutdown} \in \mathbb{R}^5$ consists of the dimensionless m-factors $m_{j,n}^{shutdown}$ ($j = I, II, III, IV$) and switching period $t_{s,n}^{shutdown}$. The objective function $J_n^{shutdown}$ is aimed to minimize the stage-wise deviation of the concentration profile $C^n(t)$ with respect to the nominal value (i.e., a zero vector) over stage n that spans the time horizon from $t_{n-1}^{shutdown}$ to $t_n^{shutdown}$. The purity constraints in Eq. (34) are used to ensure the quality of the final shutdown products. The stage-wise purities $Pu_{E,n}^{shutdown}$ and $Pu_{R,n}^{shutdown}$ are similar to those defined in the startup case (Eq. (32)):

$$Pu_{E,n}^{shutdown} = \frac{M_{B,n}^{shutdown,E}}{M_{A,n}^{shutdown,E} + M_{B,n}^{shutdown,E}},$$
$$Pu_{R,n}^{shutdown} = \frac{M_{A,n}^{shutdown,R}}{M_{A,n}^{shutdown,R} + M_{B,n}^{shutdown,R}} \tag{37}$$

where $M_{i,n}^{shutdown,E}$ and $M_{i,n}^{shutdown,R}$ are the masses of component i collected during stage n from the extract and raffinate outlets, respectively. Moreover, the operational feasibility and restrictions should be also fulfilled during shutdown, which are considered in the remaining inequality constraints. The shutdown sub-problems are solved sequentially until at the end of stage P, the total recoveries of both components reach their respective minimum threshold values:

$$Re_i^{T,shutdown} = \frac{\sum_{n=1}^{P} (M_{i,n}^{shutdown,E} + M_{i,n}^{shutdown,R})}{M_i^{Col}} \ge Re_{i,min}^{T,shutdown},$$
$$i = A, B \tag{38}$$

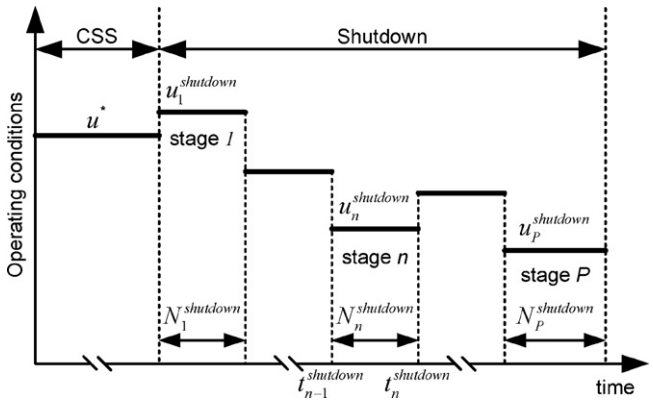

Fig. 5. Illustration of multistage shutdown strategy.

In order to assess the performance of the new transient operations quantitatively, the same set of performance criteria as that of the conventional case can be defined. For the sake of comparison, the definition of these parameters is also summarized in Table 1 for the multistage startup and shutdown cases.

5. Results and discussion

5.1. Example process

A literature example of separation of two cycloketones, cycloheptanone (less retained component A) and cyclopentanone (B) on silica gel using n-hexane:ethylacetate (85:15) as mobile phase [29] was taken to evaluate the conventional and multistage optimal startup and shutdown procedures. The adsorption behavior of the two cycloketones is characterized by the competitive Langmuir isotherm. The detailed parameters used to quantify the model

Table 2
Summary of parameters for the considered SMB process.

Column properties and operating parameters:			
Column configuration	1-1-1-1	c_i^F, $i = A, B$ [g/l]	1.25
Column dimensions [cm]	2×25	Q_{max} [ml/min]	60
ϵ	0.83	N_{NTP}	50
Adsorption isotherm coefficients:			
H_A	5.72	K_A [l/g]	0.110
H_B	7.70	K_B [l/g]	0.148

process are listed in Table 2. For this laboratory-scale example, the feed concentrations of both components were fixed identically at 1.25 g/l. The maximum allowable flow-rate Q_{max} caused by the maximum pressure drop was restricted to 60 ml/min.

5.2. Determination of CSS operating conditions

As reviewed in Section 3.1, several well-established design procedures can be used to determine the CSS operating conditions u^*. In this work, u^* was obtained by solving the following feed throughput maximization problem:

$$\max_{u^*} \quad Q_F^* \tag{39}$$

subject to:

$$\left\| C_{k+1} - C_k \right\| \le \epsilon_{css} \tag{40}$$

$$Pu_E^* \ge Pu_{E,min}, \quad Pu_R^* \ge Pu_{R,min} \tag{41}$$

$$Q_I^* \le Q_{max}, \quad Q_{III}^* \le Q_{max} \tag{42}$$

$$m_I^* - m_{II}^* > 0, \quad m_I^* - m_{IV}^* > 0, \quad m_{III}^* - m_{II}^* > 0, \quad m_{III}^* - m_{IV}^* > 0 \tag{43}$$

where $u^* = \left[m_I^*, m_{II}^*, m_{III}^*, m_{IV}^*, t_s^* \right]^T$, C_{k+1} and C_k the axial concentration profiles at the end of switching period $k+1$ and k, Pu_E^* and Pu_R^* the nominal extract and raffinate product purities required at the end of each CSS switching period, and ϵ_{css} the tolerance which controls the accuracy of CSS. The sequential solution algorithm [14,15,20,21,24] equipped with the DAE integrator DASPK3.1 [12] and a sequential quadratic programming (SQP) optimizer E04UCF from the NAG Library [30] was used to solve the CSS optimization problem. The standard dynamic simulation approach was adopted for the determination of CSS. The concentration profiles normalized with respect to the feed concentrations were used to check CSS numerically with $\epsilon_{css} = 1.0 \times 10^{-4}$. Both $Pu_{E,min}$ and $Pu_{R,min}$ were specified as 90%. The forward sensitivity analysis with respect to u^* was performed to evaluate the gradients of the purity constraints (Eq. (41)) and the other gradients were determined analytically. The obtained CSS operating conditions for the model system are reported in Table 3, and the corresponding reference concentration profile established at the end of one CSS period is shown by the thick lines in Fig. 1c for the components.

5.3. Startup strategies

For the reference process described in Section 5.1, we have examined the conventional method and multistage optimal startup with and without product purity constraint. The sequential solution approach was also used to solve the decomposed sub-problems

Table 3
CSS operating parameters for the example process.

$m_{I,\ldots,IV}^*$	[8.0485, 4.8930, 6.1933, 4.6167]	t_s^*	2.8775
Q_D^*	15.92	Q_I^*	60.00
Q_E^*	14.64	Q_{II}^*	45.36
Q_F^*	6.03	Q_{III}^*	51.39
Q_R^*	7.32	Q_{IV}^*	44.08

Flow-rates are expressed in ml/min and t_s^* in min.

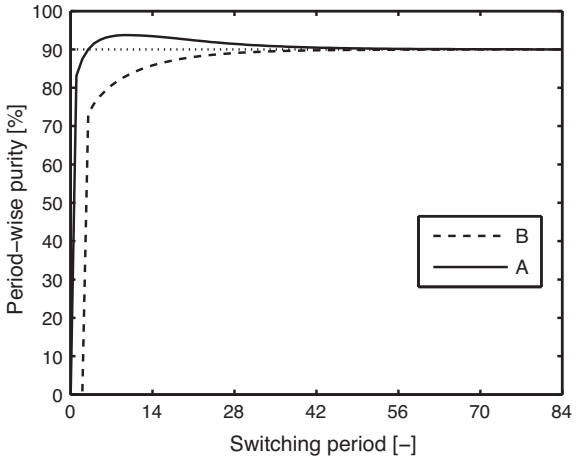

Fig. 6. Development of period-wise extract (B) and raffinate (A) purities during conventional startup. The dotted line marks the purity threshold of 90%.

formulated in Section 4.1.2. The capability of sensitivity calculation of DASPK was employed again to obtain the gradients of the objective function and purity constraints that cannot be determined analytically. The optimum solution found by E04UCF from the preceding stage was chosen as the initial guess for the sub-problem of the next stage. The number of switching periods for

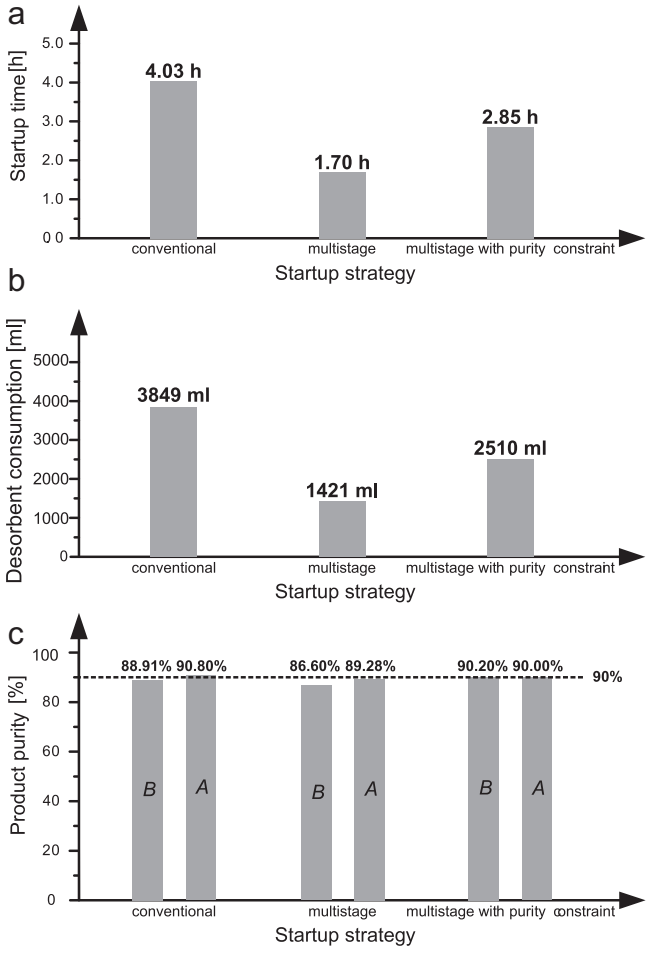

Fig. 7. Comparison of performance of different startup strategies in terms of (a) startup time, (b) desorbent consumption, and (c) extract (B) and raffinate (A) product purities. The dashed line in (c) marks the minimum purity threshold of 90%.

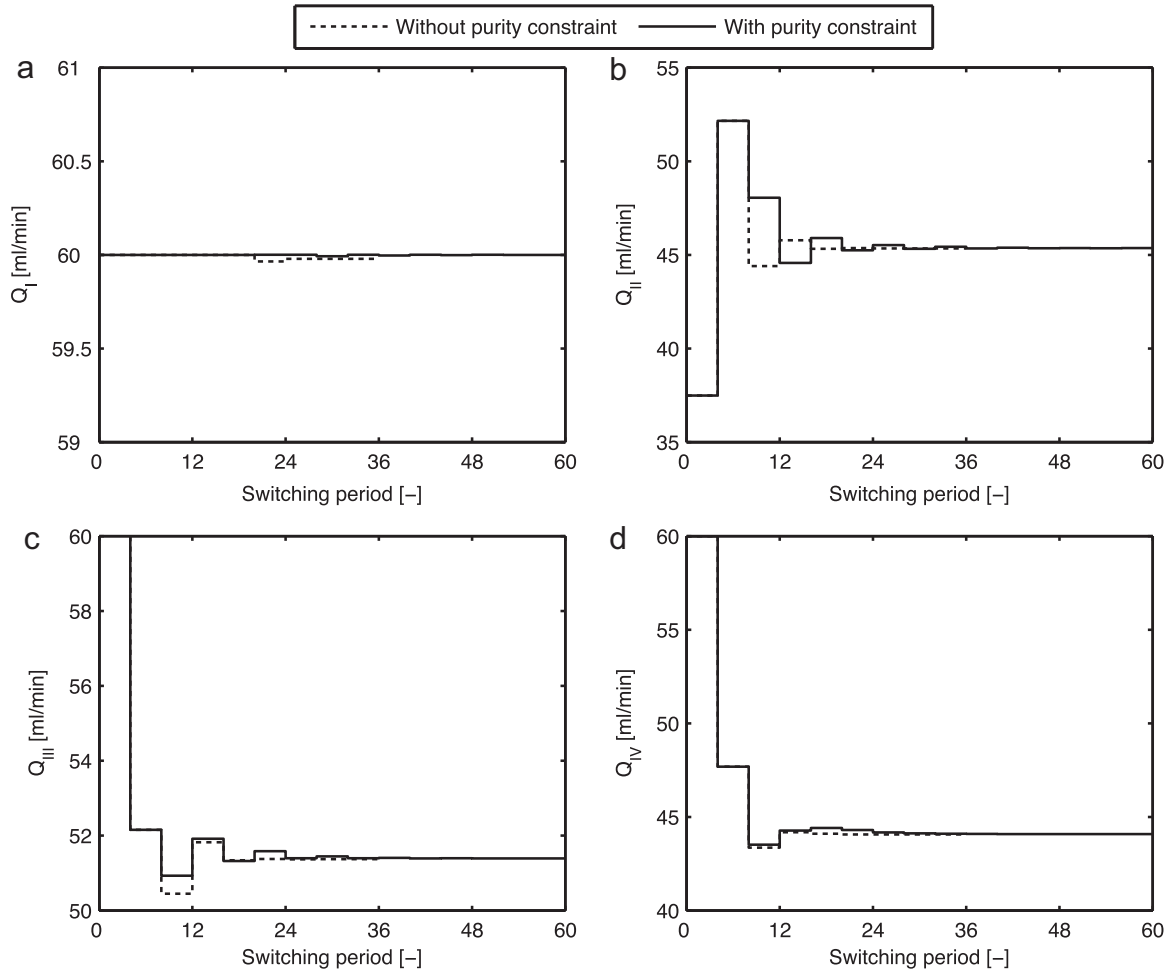

Fig. 8. Optimal startup profiles (internal flow-rates) of multistage strategies with and without purity constraint.

each stage was fixed at 4 a priori. In the scenario where purity specifications are taken into account, the same value of 90% as that required for the normal CSS products was enforced on both stage-wise extract and raffinate products. It should be pointed out that, for the example under consideration, it is infeasible for the first two stages to fulfill such high purity requirements, and both extract and raffinate streams obtained are highly dilute. Taking additional effort to guarantee reasonably good purities for these products might be feasible but is of little value, since a significant amount of evaporation cost is required. Thus, we imposed the constraints only from the third stage and discarded the outlet streams collected over the first two stages. For each startup strategy, the normalized concentration profiles were used to check the completion of startup with the same tolerance $\epsilon_{startup} = 1.0 \times 10^{-6}$. In addition, the coefficient ϵ_{reg} should be sufficiently larger than $\epsilon_{startup}$ to ensure the regularization term to be dominant before the startup ends. On the other hand, if ϵ_{reg} is too large, the optimizer would behave conservatively and the potential for finding more efficient startup regimes might be unexploited. In this work, for the case without purity constraint, we did not encounter any difficulty choosing ϵ_{reg} and a value of 1.0×10^{-3} was found to be appropriate. However, when dealing with the sub-problems with purity constraint, such value appears to be insufficient to force the operating conditions to converge to u^*, and alternatively a larger value of 5.0×10^2 was used. Note that for both cases, ϵ_{reg} remains constant over stages. A more sophisticated strategy that allows ϵ_{reg} to vary stage-wise is also possible but not considered here.

5.3.1. Conventional method

Following the conventional startup policy, the process takes 84 switching periods to achieve the reference concentration profile within the given tolerance. The resulting startup time is more than 4 h and the desorbent consumption is 3849 ml. The final extract product purity $Pu_E^{startup} = 88.91\%$, which violates the acceptable purity threshold of 90%, and the raffinate purity $Pu_R^{startup}$, on the contrary, increases to 90.80%. The results can be perfectly rationalized by examining the development of the period-wise extract and raffinate purities shown in Fig. 6. In order to avoid confusing with $Pu_E^{startup}$ and $Pu_R^{startup}$, we explicitly give the definition of the period-wise purity for the extract and raffinate:

$$Pu_{E,k}^{startup} = \frac{M_{B,k}^{startup,E}}{M_{A,k}^{startup,E} + M_{B,k}^{startup,E}}, \quad Pu_{R,k}^{startup} = \frac{M_{A,k}^{startup,R}}{M_{A,k}^{startup,R} + M_{B,k}^{startup,R}} \tag{44}$$

It is seen that although both extract and raffinate purities reach the desired value of 90% after startup, their transient behavior differs significantly from each other. For the raffinate, as time proceeds, the purity gradually converges towards the target with values obviously higher than 90% except those of the initial very few periods. The on-spec raffinate startup product therefore results. By contrast, the extract purity is consistently lower than 90% over the startup stage, thus making it impossible to achieve an on-spec extract startup product.

For this startup scheme, the effect of feed concentration on the startup product purity has been also investigated. For this

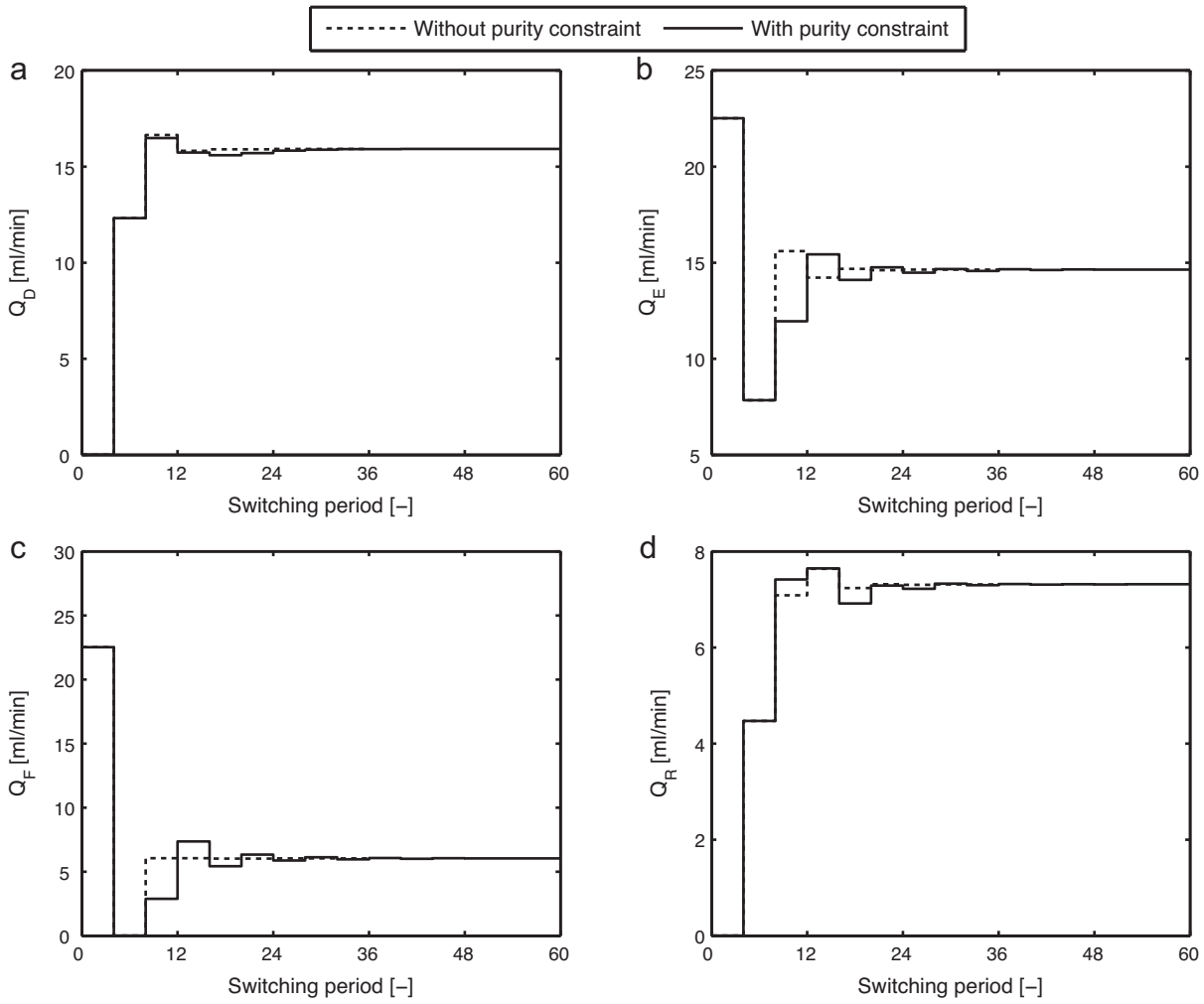

Fig. 9. Optimal startup profiles (external flow-rates) of multistage strategies with and without purity constraint.

purpose, the feed concentrations of both components were altered from those of the reference system and are summarized in Table 4. For each process of different feed concentrations, the optimization problem presented in Section 5.2 was solved to find the corresponding CSS operating conditions. The modified systems were then started up in the conventional way to reach their respective reference profiles. In each case, the purities of extract and raffinate products collected over the startup period are reported in Table 4. As expected, for the cases examined, although the raffinate purity remains higher than 90%, the extract purity, however, always deviates adversely from the desired value. The extent of such deviation becomes more significant at higher feed concentrations. For the system with the feed concentrations of 2.5 g/l, the extract purity drops up to 88.79%. The results obviously reveal that the conventional scheme has no ability to ensure on-spec startup products.

Table 4
Purities of extract and raffinate products obtained during conventional startup for systems with different feed concentrations.

c_i^F, $i = A, B$ [g/l]	0.55	1.25	2.0	2.5
$Pu_E^{startup}$ [%]	89.12	88.91	88.83	88.79
$Pu_R^{startup}$ [%]	90.38	90.80	90.98	91.05

5.3.2. Multistage optimal operation

For the same process, when using the optimal startup procedure, the total number of switching periods required to reach the reference profile is reduced from 84 to 36 (9 stages with four switching periods per stage). If the purity constraint of 90% is explicitly imposed on both products from the third stage, the process needs 15 stages and totally 60 switching periods to complete the startup. A detailed comparison of the conventional and multistage startup strategies in terms of startup time, desorbent consumption and product purity is illustrated in Fig. 7a, b and c, respectively. The new startup regime without purity constraint allows the process to achieve a reduction of 58% in startup time and a saving of 63% in desorbent usage, compared to the normal startup mode. However, both product purities are below the specified requirements and even a bit lower than those of the conventional approach. By contrast, for the case with purity constraint, the on-spec production can be successfully performed over startup. But note that such a guarantee of product quality comes at the expense of a slight increase of startup time and desorbent consumption with respect to the case without quality constraint. In spite of this, however, significant benefits are still observed for both performance parameters from Fig. 7a and b. In this case, the startup time and desorbent consumption can be reduced by 29% and 35%, respectively. The results also reflect that there exists a tradeoff between the rapidity of startup and product quality. It should be pointed out that the desorbent consumption is not explicitly included in the objective function. The achieved

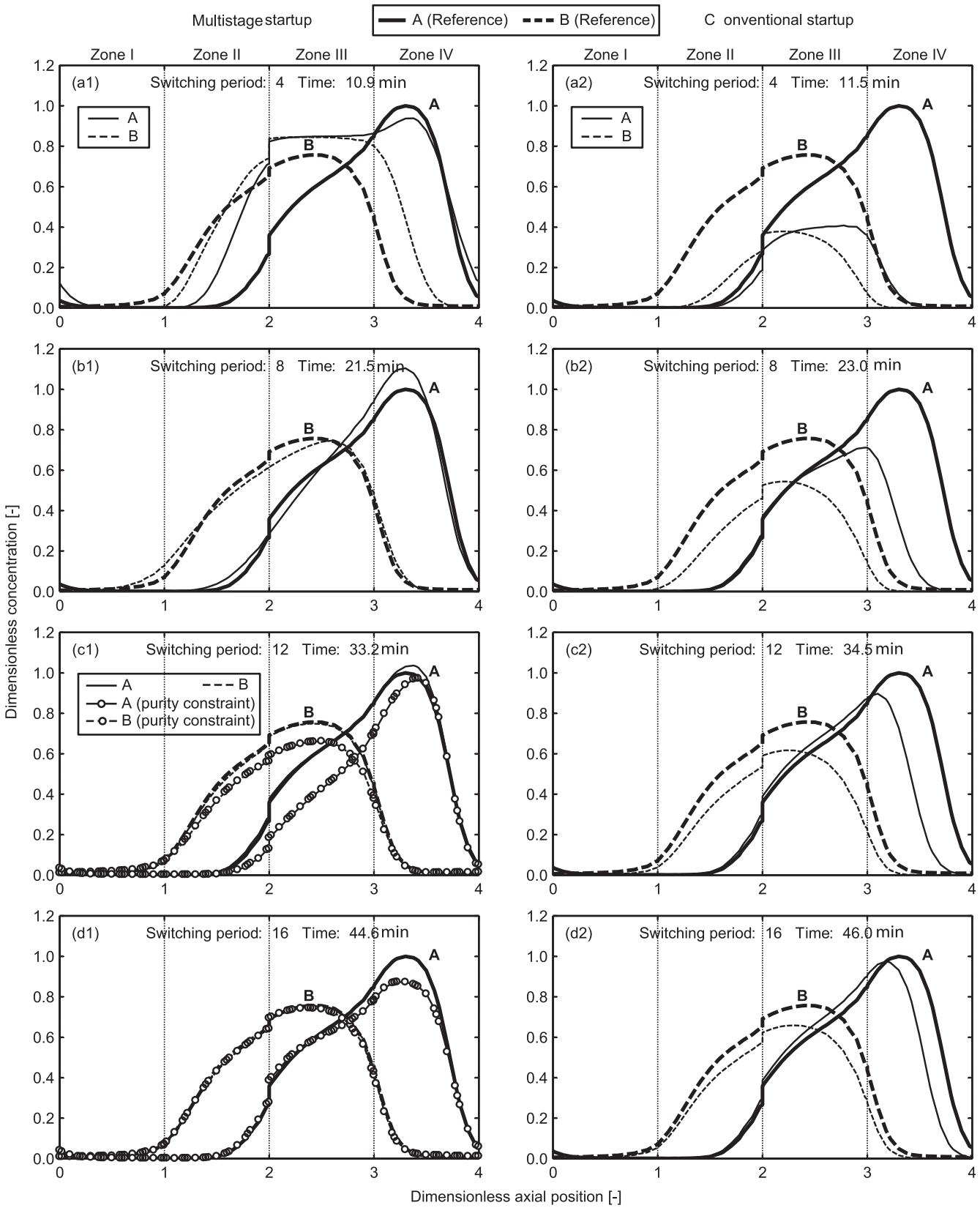

Fig. 10. Comparison of development of axial concentration profiles with different startup strategies. The profiles are taken at the end of (a) stage 1 (switching period 4), (b) stage 2 (switching period 8), (c) stage 3 (switching period 12), and (d) stage 4 (switching period 16). For the multistage regime with purity constraint, since the profiles at the end of stages 1 and 2 are the same as those obtained without constraint, they are not plotted in sub-graphs (a1) and (b1) for simplicity. The profiles of each component are normalized with respect to its feed concentration.

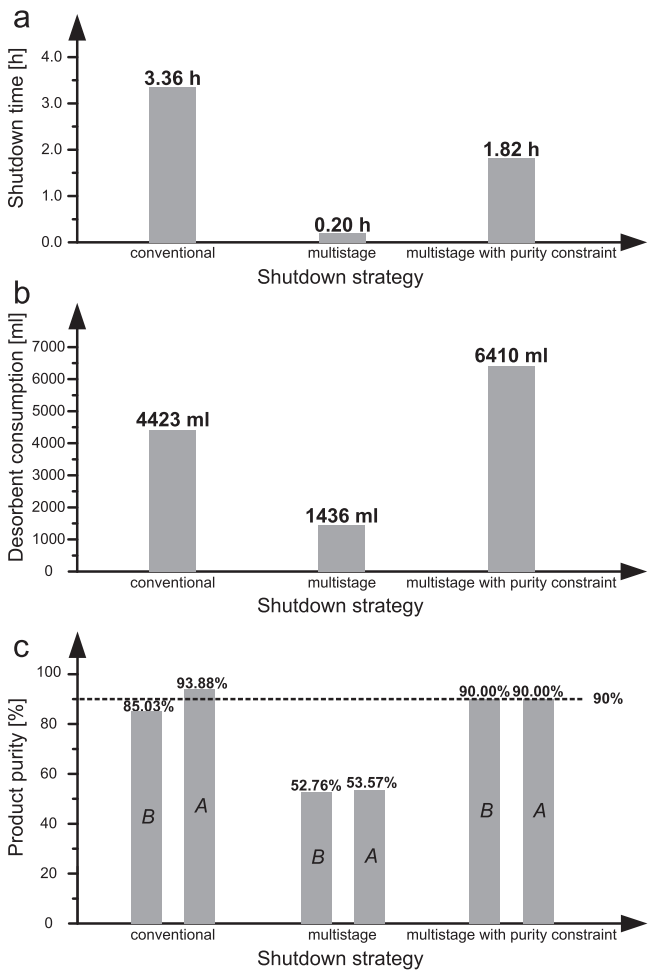

Fig. 11. Comparison of performance of different shutdown strategies in terms of (a) shutdown time, (b) desorbent consumption, and (c) extract (B) and raffinate (A) product purities. The dashed line in (c) marks the minimum purity threshold of 90%.

reduction in desorbent usage is a side benefit of minimizing startup time.

The optimal startup operating conditions obtained for the two cases in terms of internal and external flow-rates are demonstrated in Figs. 8 and 9, respectively. Let us first take a closer look at the case without purity constraint. It is seen that the flow-rates Q_I, Q_{III} and Q_{IV} reach the upper bound of 60 ml/min simultaneously in the first stage (see Fig. 8a, c, d), whereas a relatively lower value of 37.48 ml/min is achieved by Q_{II} (Fig. 8b). As a result, over the same stage $Q_D = Q_R = 0$ and $Q_E = Q_F = 22.52$ ml/min (see Fig. 9). From Fig. 9c, it is also noted that the value of Q_F is more than 3.5 times higher than its CSS value of 6.03 ml/min. The quantitative observations for Q_D and Q_F clearly reveal useful operating guidelines for accelerating attainment of the desired CSS profile: the feed flow-rate should be operated at a higher value than the nominal one to load the fresh mixture into the columns quickly, while the desorbent must be shut off to avoid dilution. On the other hand, the results for the raffinate and extract flow-rates are also rather enlightening. For the reference process, it is found that the raffinate begins to elute out in the first switching period. By contrast, the extract cannot be withdrawn until a few periods have elapsed. Thus, the behavior that $Q_R = 0$ aims to prevent the raffinate accumulated inside the columns eluting out of the unit; a high value of Q_E implies that the process attempts to throw away the solvent residing in the system and to reduce dilution.

Over the second stage, Q_{II} undergoes a dramatic increase up to 52.15 ml/min and Q_{III} on the contrary quickly drops from 60 ml/min to the same value. This causes the feed flow-rate Q_F to decrease to zero. Obviously, such a control profile of Q_F is intended to avoid the potential overload of the columns. Moreover, Q_D and Q_R rise from zero to 12.32 ml/min and 4.47 ml/min, respectively. As the stage further increases, the flow-rates shown in Figs. 8 and 9 gradually converge towards their CSS values. After about 5 stages, they have almost reached the nominal values, which reflects that the first several stages play a more dominant role in improving the startup performance. Note that the flow-rate in zone I always remains at 60 ml/min during the entire startup process.

For the case with purity constraint, the optimal startup regime over the initial two stages is the same as that of the previous scenario. This is because no stage-wise purity requirements are specified on these stages, as already pointed out, and the same two startup optimization sub-problems were solved in this case. Once the extract and raffinate purity constraints are explicitly enforced from the third stage, the obtained optimal operating conditions exhibit a different behavior, as can be seen from Figs. 8 and 9. In the case of the internal flow-rates, for example, it is readily noted from Fig. 8 that such a difference with respect to the previous case is particularly striking in Q_{II} and Q_{III}, but much less noticeable in Q_I and Q_{IV}. This can be explained as follows: typically, Q_{II} and Q_{III} have a more significant impact on the extract and raffinate purities, respectively. Therefore, when the purity constraints are imposed, the optimizer chooses to adjust them in order to avoid the violation of the constraints.

The development of axial concentration profiles for the multistage strategies over the first four stages is illustrated in the left column of Fig. 10. Note that for the scenario with purity constraint, since the profiles at the end of stages 1 and 2 are the same as those obtained without constraint, they were omitted for simplicity in Fig. 10a1 and b1, respectively. For comparison purposes, the results of the conventional startup at the end of switching periods 4, 8, 12, and 16 are also plotted in sequence in the right column of the same figure. To allow for fair comparison, the corresponding absolute time elapsed since the beginning of the startup operation is given explicitly in each sub-graph of Fig. 10. It can be observed that the new startup regime without purity constraint enables the process to achieve the fastest convergence to the reference profile, although the case considering the quality constraints also clearly outperforms the conventional approach. At the end of stage 1, the multistage scheme allows to establish a concentration plateau more than two times higher than that of the normal startup (see Fig. 10a1, a2). In this case, the raffinate (A) concentration in zones II and III and extract (B) concentration in zones III and IV are even higher than the corresponding reference profiles. For both components, the axial profiles approximate the reference ones rather well at the end of the second stage (Fig. 10b1), and even better than those do at the end of switching period 16 in the conventional case (Fig. 10d2). Once the stage-wise purity of 90% is required from the next stage, the development of the profiles differs significantly from that without purity specifications. By the end of stage 4, the profiles in the previous case have already perfectly converged. However, fulfilling the purity requirements results in a relatively slower convergence rate, as can be seen in Fig. 10c1 and d1. In addition, it is noted from Fig. 10c1 that the concentration fronts of component A in zones II and III are shifted to the right relative to those of the previous case. This interesting observation can be elucidated as follows. In Section 5.3.1 we have shown the period-wise purity profiles (see Fig. 6). The profiles, although obtained with the conventional startup, to a certain extent also reflect that respecting the required stage-wise purity of 90% might be more non-trivial for the extract than for the raffinate. Such a variation of the shape of the front can reduce the

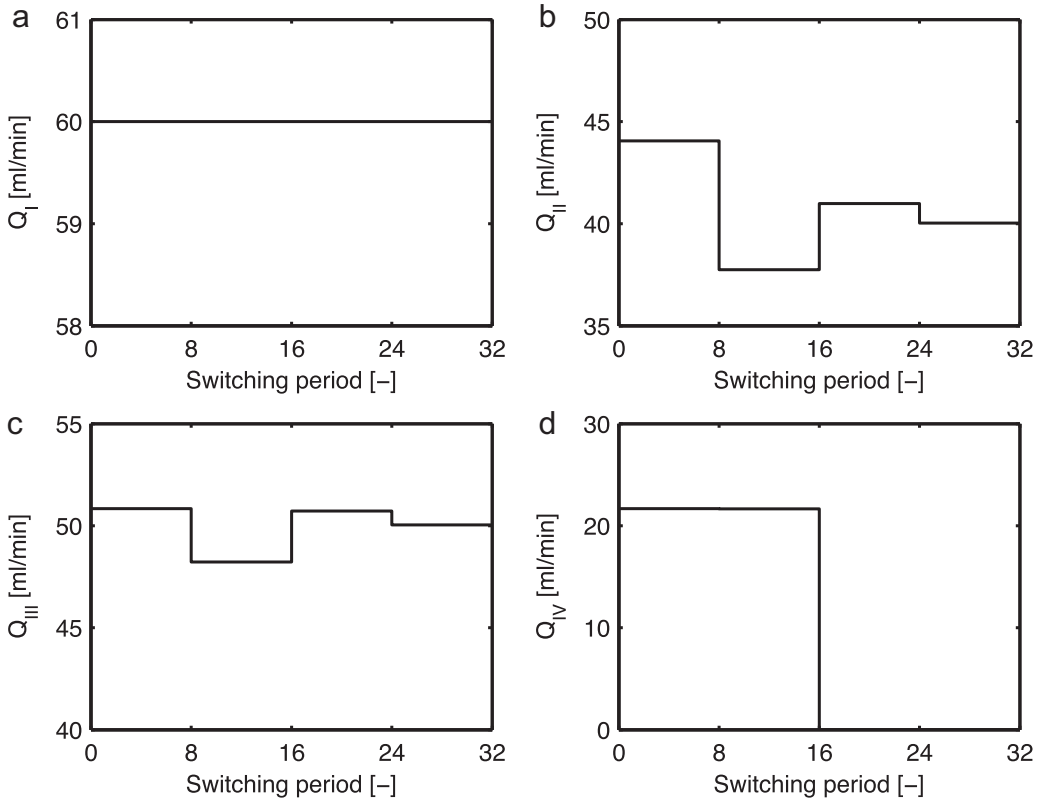

Fig. 12. Optimal internal flow-rate profiles for the multistage shutdown strategy with purity constraint.

impurity present in the extract product and help it satisfy the purity requirement.

5.4. Shutdown strategies

To study the shutdown issue, the amount of each component accumulated in the columns at CSS is required, which also shows a periodic behavior. For convenience, the shutdown procedure is assumed to start only after some full CSS period is completed. With this assumption, the accumulated value can be readily calculated by subtracting the amount collected from both extract and raffinate outlets from the total amount supplied to the system until the end of this switching period. The conventional startup approach was used to determine the results. For the model separation, the total masses retained in the columns are 0.2258 g and 0.2293 g for component A and B, respectively. The primary goal of a shutdown procedure is to recover these holdups in an efficient way. For the multistage regime, a sequence of decomposed sub-problems presented in Section 4.2 was solved by the sequential approach. The number of switching periods involved in each stage was specified as eight. In the case that considers the purity specifications, the same requirement of 90% as in the startup case was imposed on the stage-wise shutdown products. For each shutdown scheme examined, once the total recoveries of both components defined in Eq. (38) reach the minimum threshold $Re_{i,min}^{T,shutdown} = 99.95\%$ ($i = A, B$), the shutdown phase is considered to be terminated.

A systematic comparison of performance of different shutdown strategies in terms of the shutdown time, desorbent consumption and product purity is demonstrated in Fig. 11a, b, and c, respectively. The conventional scheme needs 70 switching periods and 3.36 h to complete the shutdown process, during which the total amount of desorbent consumed is 4423 ml. In this case, it is observed from Fig. 11c that an off-spec extract product of purity of 85.03% is produced, although the raffinate purity is higher than 90%. The quantitative results indicate that the conventional shutdown is not able to ensure the quality of the final products either. With the aid of the proposed shutdown regime, the same process takes only one stage (eight switching periods) and totally 0.20 h to shut down and the desorbent consumption can be saved by 68%. Such rapid shutdown is achieved at the sacrifice of the product quality. Both product purities are just around 55% and even lower than those of the conventional mode. Once the purity specification of 90% is required, an on-spec production of the extract and raffinate products can be obtained during shutdown, as can be seen from Fig. 11c. However, higher desorbent consumption and longer shutdown time result, compared to those of the previous case. In this last scenario, four stages and 1.82 h are spent to shut down the SMB unit. In contrast to that of the conventional operation, the total time is shortened by 45%. The amount of desorbent used, however, tends to be increased to some degree.

For the optimal operating conditions, it is found that in the case without purity constraint, both Q_I and Q_{III} touch the allowable upper limit of 60 ml/min, while $Q_{IV} = 0$ ml/min and Q_{II} also approaches zero (0.32 ml/min). As a result, $Q_D = Q_R = 60$ ml/min and $Q_E = Q_F = 59.68$ ml/min. The results well approximate one extreme case where $Q_I = Q_{III} = Q_D = Q_E = Q_F = Q_R = 60$ ml/min and $Q_{II} = Q_{IV} = 0$ ml/min, and mean that during the shutdown process, two purge paths are formed to clean the columns and to recover the retained components. Here, a zero flow-rate in both zones II and IV aims at isolating the columns being washed from those to be treated. The purge flows Q_D and Q_F operated at the maximum flow-rate value enable the process to wash the holdups out of the columns efficiently.

The optimal internal flow-rate profiles with purity constraint are illustrated in Fig. 12. It can be seen that although the optimal Q_I also remains at the upper bound, the other flow-rates

exhibit different behavior in contrast to that without purity constraint. In particular, significant variation in both Q_{II} and Q_{III} can be observed, which aims to fulfill the purity constraints enforced on each stage. Additionally, the optimal profile of Q_{IV} is not kept at zero as before, but drops from 21.66 ml/min to zero from the third stage. The external flow-rates also behave distinctly from those in the previous case. For the two purge flows, Q_D does not increase to 60 ml/min until at the third stage; Q_F ranges only from 6 to 11 ml/min and becomes significantly smaller compared to the previous result.

6. Summary and future work

The periodic behavior and complex nonlinear process dynamics of SMB chromatography poses a significant challenge for the formulation and solution of its optimal transient operation problem. In this paper, the multistage optimal startup and shutdown schemes were suggested. To guarantee the numerical solvability of the resulting dynamic optimization problems, a specially tailored decomposition solution strategy was employed. An existing literature separation example with nonlinear competitive Langmuir isotherm was considered as a case study. The feasibility of the solution algorithm was demonstrated and the performance achievable by the conventional and multistage operation regimes was evaluated in detail. It is shown that for the case without product quality constraints, the new policies not only drastically reduce transient duration, but also lead to significant savings in desorbent consumption. Another obvious advantage of our multistage approach lies in its ability to optimize transient performance while respecting product quality requirements. This strength enables on-spec production of both extract and raffinate products during the startup and shutdown periods, which cannot be guaranteed with the conventional methods. The result could be extremely attractive for the production of valuable chemical products where either discarding or reprocessing off-spec transient products is highly undesirable. The efficient startup and shutdown strategies presented in this paper are not only advantageous for continuous large-volume purifications, but also expand the applicability of SMB to small batch productions.

A detailed experimental validation of the theoretical optimal policies is currently under way. Furthermore, development of efficient solution algorithms for the optimal transient operation of such periodic adsorption process still remains an open question. Our future efforts will concentrate on the exploration of alternative solution approaches that can avoid decomposition, taking modeling error and parameter uncertainty into account, and application of the proposed concept to multi-column gas adsorption processes, such as pressure swing adsorption (PSA).

Acknowledgements

Y. Kawajiri was supported partially by the Alexander von Humboldt Research Fellowship. Support from Knauer Wissenschaftliche Gerätebau GmbH (Berlin), Fonds der Chemischen Industrie (Köln) and the European Union research project ("IntEnant": FP7-NMP2-SL2008-214129) is gratefully acknowledged.

References

[1] A. Rajendran, G. Paredes, M. Mazzotti, J. Chromatogr. A 1216 (2009) 709.
[2] B.G. Lim, C.B. Ching, Sep. Technol. 6 (1996) 29.
[3] Y. Xie, S.Y. Mun, N.-H.L. Wang, Ind. Eng. Chem. Res. 42 (2003) 1414.
[4] Y.-S. Bae, J.-H. Moon, C.-H. Lee, Ind. Eng. Chem. Res. 45 (2006) 777.
[5] Y.-S. Bae, K.-M. Kim, J.-H. Moon, S.-H. Byeon, I.-S. Ahn, C.-H. Lee, Sep. Purif. Technol. 62 (2008) 148.
[6] N. Abunasser, P.C. Wankat, Ind. Eng. Chem. Res. 43 (2004) 5291.
[7] R.C.R. Rodrigues, J.M.M. Araújo, M.F.J. Eusébio, J.P.B. Mota, J. Chromatogr. A 1142 (2007) 69.
[8] G. Zenoni, M. Pedeferri, M. Mazzotti, M. Morbidelli, J. Chromatogr. A 888 (2000) 73.
[9] S. Li, Y. Kawajiri, J. Raisch, A. Seidel-Morgenstern, in: Proc. of the 9th International Symposium on Dynamics and Control of Process Systems, Leuven, Belgium, 2010.
[10] Z. Ma, N.-H.L. Wang, AIChE J. 43 (1997) 2488.
[11] G. Guiochon, A. Felinger, D.G. Shirazi, A.M. Katti, Fundamentals of Preparative and Nonlinear Chromatography, Academic Press, Elsevier, Amsterdam, 2006.
[12] S. Li, L. Petzold, Technical Report, University of California, Santa Barbara, CA, USA, 1999.
[13] M. Mazzotti, G. Storti, M. Morbidelli, J. Chromatogr. A 769 (1997) 3.
[14] G. Dünnebier, K.-U. Klatt, Comput. Chem. Eng. 23 (1999) S195.
[15] G. Dünnebier, J. Fricke, K.-U. Klatt, Ind. Eng. Chem. Res. 39 (2000) 2290.
[16] Z. Zhang, K. Hidajat, A.K. Ray, M. Morbidelli, AIChE J. 48 (2002) 2800.
[17] Y. Kawajiri, L.T. Biegler, AIChE J. 52 (2006) 1343.
[18] J.M.M. Araújo, R.C.R. Rodrigues, J.P.B. Mota, J. Chromatogr. A 1132 (2006) 76.
[19] A. Toumi, S. Engell, M. Diehl, H.G. Bock, J. Schlöder, Chem. Eng. Process. 46 (2007) 1067.
[20] A. Toumi, S. Engell, O. Ludemann-Hombourger, R.M. Nicoud, M. Bailly, J. Chromatogr. A 1006 (2003) 15.
[21] A. Toumi, F. Hanish, S. Engell, Ind. Eng. Chem. Res. 41 (2002) 4328.
[22] Z. Zhang, M. Mazzotti, M. Morbidelli, J. Chromatogr. A 1006 (2003) 87.
[23] M.S.G. García, E. Balsa-Canto, J.R. Banga, A. Vande Wouwer, Ind. Eng. Chem. Res. 45 (2006) 9033.
[24] S. Li, Y. Kawajiri, J. Raisch, A. Seidel-Morgenstern, J. Chromatogr. A 1217 (2010) 5337.
[25] S. Li, Y. Kawajiri, J. Raisch, A. Seidel-Morgenstern, J. Chromatogr. A 1217 (2010) 5349.
[26] Z. Zhang, M. Mazzotti, M. Morbidelli, Korean J. Chem. Eng. 21 (2004) 454.
[27] Y. Kawajiri, L.T. Biegler, Ind. Eng. Chem. Res. 45 (2006) 8503.
[28] G. Wozny, P. Li, Comput. Chem. Eng. 28 (2004) 253.
[29] H. Schramm, M. Kaspereit, A. Kienle, A. Seidel-Morgenstern, J. Chromatogr. A 1006 (2003) 77.
[30] The NAG Fortran Library Manual. Mark 18, vol. 5, NAG Ltd., Oxford, 1997.